ChemComm

COMMUNICATION

View Article Online
View Journal | View Issue

Cite this: *Chem. Commun.*, 2020, **56**, 12037

Received 1st July 2020,
Accepted 3rd September 2020

DOI: 10.1039/d0cc04559d

rsc.li/chemcomm

Engineering macrocyclic high performance pentagonal bipyramidal Dy(III) single-ion magnets†

Angelos B. Canaj, [a] Sourav Dey, [b] Claire Wilson, [a] Oscar Céspedes, [c] Gopalan Rajaraman *[b] and Mark Murrie *[a]

We generate a new air-stable *pseudo*-D_{5h} Dy(III) Single-Molecule Magnet (U_{eff} = 1108 K, T_B = 14 K) by combining a weak equatorial ligand field from a macrocyclic L^{N5} ligand with a strong axial ligand field. Based on our synthetic blueprint, we use *ab initio* calculations to show the vast scope for macrocyclic engineering of magnetic anisotropy.

Molecular systems which display the ability to retain magnetisation, in the absence of an external magnetic field, resulting in the appearance of magnetic memory of molecular origin, are known as Single-Molecule Magnets (SMMs).[1] Lanthanide-based SMMs are often associated with large magnetic moments and large magnetic anisotropy. In 4f-SMMs, the energy barrier to reorientation of the magnetisation (U_{eff}) is strongly determined by the control of the coordination environment at the level of a single metal ion.[2] Specifically, the use of the Dy(III) ion in targeted coordination environments that promote strong uniaxial symmetry stabilizes the largest $m_J = \pm 15/2$ ground state and gives a large separation from the excited m_J states.[2] Monometallic complexes with axial symmetry such as square antiprismatic,[3] trigonal bipyramidal,[4] pentagonal bipyramidal,[5,6] and hexagonal bipyramidal,[7,8] are an effective way to favour slower relaxation of the magnetisation. Furthermore, sandwich type ligands (*e.g.* cyclopentadienyl (Cp) anionic ligands), have generated organometallic compounds with impressive blocking temperatures showing coercivity up to 30 K,[9] 48 K,[10] 55 K,[11] 60 K,[12] 66 K[13] and 80 K.[14] Additionally, a unique family of Ln-SMMS are the endohedral metallofullerenes (EMFS).[15]

We have explored how the ligand electronics can tune SMM properties[5,7,16,17] and recently first introduced a blueprint for engineering strong uniaxial magnetic anisotropy for Dy(III) ions in a hexagonal bipyramidal geometry,[7] boosting the magnetisation reversal barrier from ~50 K[18] to ~1100 K, by using the macrocyclic ligand $\mathbf{L^{N6}}$ (Scheme 1 left). Implementing further the flexibility of our synthetic approach towards the engineering of new quasi-D_{nh} systems, we demonstrate the isolation of a new Single-Ion Magnet (SIM) with pentagonal bipyramidal geometry, $[Dy^{III}(\mathbf{L^{N5}})(Ph_3SiO)_2](BPh_4)\cdot CH_2Cl_2$ (**1**). Compound **1** shows out-of-phase peaks in the ac susceptibility up to 80 K under zero dc field, a high magnetization reversal barrier of 1108 K and hysteresis, M(H), loops open up to 14 K, measured at an average sweep rate of 0.01 T s^{-1} (see Table S1, ESI†). **1** belongs to a small group of pentagonal bipyramidal complexes that are both air-stable and have a U_{eff} above 1000 K (Table S1, ESI†). In our carefully designed step-by-step synthetic approach we first targeted the formation of a weak N5-pentagonal plane by employing the macrocyclic $\mathbf{L^{N5}}$ ligand (Scheme 1, right), unused in 4f chemistry, formed from 2,6-diacetylpyridine and *N*,*N*′-bis-(3-aminopropyl)-ethylendiamine.[19] We then used the anion of triphenylsilanol, Ph_3SiO^-, as stronger anionic donors at both axial positions to generate the pentagonal bipyramidal architecture (Fig. 1).

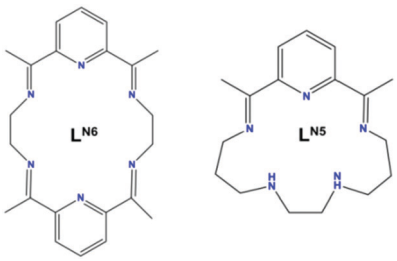

Scheme 1 The macrocyclic ligand $\mathbf{L^{N6}}$ (left)[7] and $\mathbf{L^{N5}}$ (right).

Importantly, our synthetic strategy offers vast synthetic flexibility for carefully engineering the equatorial crystal field in order to (i) further improve the relaxation dynamics and (ii) to target the isolation of new quasi-D_{nh} systems with enhanced magnetic anisotropy. In a quest to identify new promising directions towards high temperature SMMs we also investigate the new *in silico* models **1-N3O2** and **1-O5** (*vide infra*), inspired

[a] *School of Chemistry, University of Glasgow, University Avenue, Glasgow, G12 8QQ, UK. E-mail: mark.murrie@glasgow.ac.uk*
[b] *Department of Chemistry, Indian Institute of Technology Bombay, Powai, Mumbai, Maharashtra, 400076, India. E-mail: rajaraman@chem.iitb.ac.in*
[c] *School of Physics and Astronomy, University of Leeds, Leeds LS2 9JT, UK*

† Electronic supplementary information (ESI) available: Experimental section, magnetic studies, crystallographic details, *ab initio* studies. CCDC 2000246. For ESI and crystallographic data in CIF or other electronic format see DOI: 10.1039/d0cc04559d

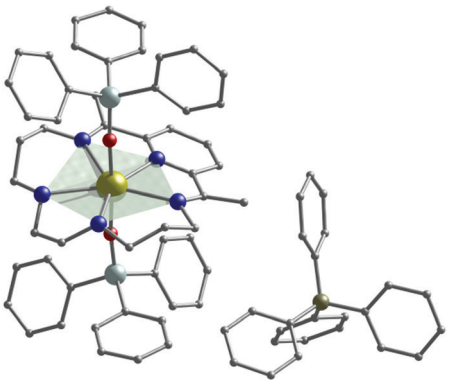

Fig. 1 Molecular structure of **1** with two Ph_3SiO^- axial ligands and the polydentate ligand $\mathbf{L^{N5}}$ in the equatorial plane, highlighted in green. Dy, gold; O, red; N, blue; Si, light turquoise; C, gray; B, dark yellow. Hydrogen atoms, solvent molecules and disorder components are omitted for clarity.

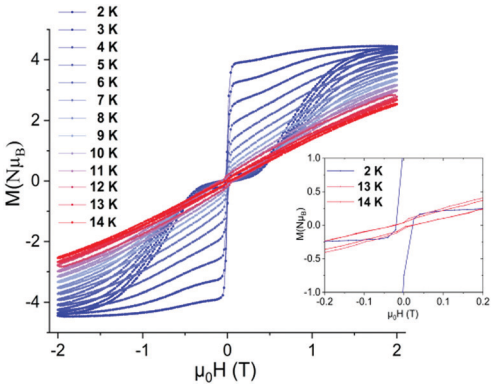

Fig. 2 Powder magnetic hysteresis measurements for **1** with an average sweep rate of 0.01 T s^{-1}. Inset: *M*(H) loops around zero field region open up to 14 K.

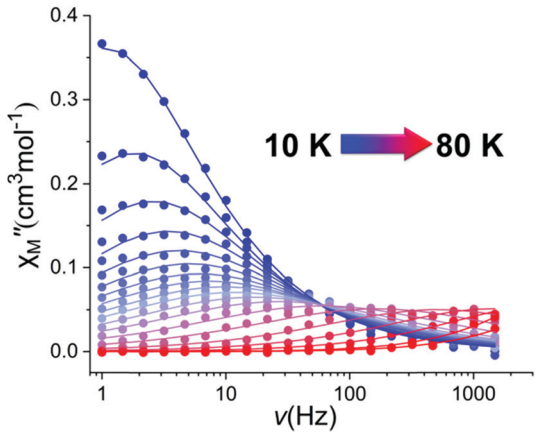

Fig. 3 Plots of χ_M'' (ν) in zero applied dc field in the temperature range of 10–80 K for **1**.

by **1**. From our systematic study, we find that the proposed *in silico* models are extremely promising as new target systems and have the potential to show improved SMM properties, with the magnetisation reversal barrier boosted up to *ca.* 1400 K and 1800 K, respectively (*vide infra*).

Compound **1** (Fig. 1) crystallises in the triclinic space group $P\bar{1}$ (Table S2, ESI†) with the asymmetric unit containing two crystallographically independent molecules with a Dy···Dy distance of 11.667 Å. Both Dy(III) centres are found in an axially compressed pentagonal bipyramidal geometry, as confirmed *via* SHAPE analysis (see Table S4 and Fig. S3, ESI†).[20] Two Ph_3SiO^- ligands occupy the axial positions providing the shortest axial Dy–O bond lengths of 2.157(3) Å and 2.136(4) Å for Dy1A and 2.161(4) Å and 2.158(4) Å for Dy1B (see Table S3 and Fig. S2, ESI†). In addition, the axial O–Dy–O angle is 176.54(15)° and 173.13(15)° for Dy1A and Dy1B, respectively. In the equatorial plane of the $\mathbf{L^{N5}}$ ligand (Fig. S2, ESI†) the Dy–N bonds fall in the range of 2.400(5)–2.570(5) Å for Dy1A and 2.457(5)–2.564(5) Å for Dy1B (Table S3, ESI†).

The static dc magnetic susceptibility and magnetization measurements for complex **1** are shown in the ESI† (Fig. S4 and S5). Upon cooling the $\chi_M T$ profile of **1** decreases steadily from the room temperature value of 14.1 $cm^3\ mol^{-1}$ K to a value of 13.05 $cm^3\ mol^{-1}$ K at 10 K followed by a sharp drop below 10 K (Fig. S4, ESI†). The field-cooled (FC) and zero-field cooled (ZFC) magnetic susceptibility (Fig. S6, ESI†) diverge at 7 K for **1** with the maximum observed at ~5 K, indicative of a magnetic blocking temperature, T_B.[21] The magnetic hysteresis measurements, *M*(H) loops, performed on a microcrystalline powder sample of **1** remain open up to 14 K, measured at a sweep rate of 0.01 T s^{-1} (Fig. 2 and Fig. S7, ESI†). The characteristic waist-restricted shape of the loops is strongly affected by the faster relaxation around zero field, due to the presence of unsuppressed Quantum Tunnelling of the Magnetisation (QTM).[3]

Alternating current (ac) susceptibility measurements were performed in order to investigate the magnetic relaxation in **1** (Fig. 3 and Fig. S8–S11, ESI†). Under zero dc field, the out-of-phase χ_M'' susceptibility data exhibit well-defined maxima, clearly observable at temperatures up to 80 K (Fig. 3 and Fig. S8, ESI†), indicative of slow magnetic relaxation and a high magnetisation reversal barrier. The magnetisation relaxation times, τ, were extracted by fitting the Argand plots of χ_M'' *vs.* χ_M' using the generalized Debye model (Fig. S11, ESI†).[22] The α-parameters found are in the range of 0.17–0.43 (2–80 K) showing a relatively wide distribution of relaxation times. The τ^{-1} *vs.* *T* data were fitted using the equation $\tau^{-1} = \tau_{QTM}^{-1} + CT^n + \tau_0^{-1}\exp(-U_{eff}/T)$, in which *C* and *n* are the parameters of the Raman process and τ_{QTM} is the rate of QTM.[3,21] The best fit gives a magnetisation reversal barrier U_{eff} = 1108 K, $\tau_0 = 1.56 \times 10^{-11}$ s, *n* = 2.05, *C* = 0.03 $K^{-n}\ s^{-1}$, τ_{QTM} = 0.5 s, under zero dc field (Fig. S12, ESI†). The values of τ_0, *C* and *n* are within the commonly observed range for Dy(III) SMMs.[3] The exponent *n* of the Raman process has a smaller value than expected for a Kramers ion (*i.e.*, *n* = 9) suggesting the presence of Raman processes involving optical acoustic phonons.[22]

Ab initio calculations on **1**, using the CASSCF/RASSI-SO/SINGLE_ANISO approach implemented in MOLCAS 8.2 (see ESI†),[23] reveal that the eight Kramers Doublets (KDs) span an energy range of ~1520 K. Inspection of the calculated *g*-tensors (Table S5, ESI†) show a highly anisotropic ground state

(m_J = ±15/2) with strong axiality (g_{zz} = 19.979, g_{xx}, g_{yy} = 0.001 for Dy1A and g_{zz} = 19.984, g_{xx}, g_{yy} = 0.000 for Dy1B). The main anisotropy axis in **1** is nearly collinear with the shortest O–Dy–O bonds, stabilised by the stronger donor Ph_3SiO^- ligands located above and below the equatorial plane of the $\mathbf{L^{N5}}$ ligand (Fig. 1 and Fig. S13, ESI†).

The first excited state (m_J = ±13/2), located at ~600 K (594 K for Dy1A and 602 K for Dy1B) and the second excited state (m_J = ± 11/2) located at ~1040 K (1033 K for Dy1A and 1040 K for Dy1B) are also axial in nature (Fig. S14 and Table S5, ESI†). The maximum calculated relaxation barrier, U_{cal}, for compound **1** is estimated at ~1040 K; in excellent agreement with the experimentally determined magnetisation reversal barrier (U_{eff}) of 1108 K found in zero dc field.

One can imagine changing the planarity and rigidity of the $\mathbf{L^{N5}}$ macrocycle by using different building blocks (or the application of pressure) to allow access to new *pseudo*-D_{5h} environments. Our ongoing efforts are focused on fully exploring the vast synthetic flexibility in the design that our approach offers in order to improve the relaxation dynamics. In this regard, the LoProp[26] charges on **1**, computed using the CASSCF wavefunction, show that the negative charges at the secondary amine –NH– groups are of similar magnitude to those found for the axial oxygen atoms (Fig. S15, ESI†). Hence, replacing the secondary amine –NH– groups with tertiary amines has the potential to result in smaller negative LoProp charges in the equatorial plane, which may have a significant impact on further improving the magnetic properties of **1**.

Furthermore, the ability to discover promising new candidate systems that have the potential to show improved SMM properties and could be targeted by experimental chemists is of key importance. Following on from the insight gained from the LoProp charges, using **1** as a blueprint we have created the *in silico* model systems **1-N3O2** and **1-O5** (Fig. S16 and S17, ESI†). In the new model systems we examine how changes in the first coordination sphere of **1**, at the equatorial positions, affect the magnetic anisotropy. In both model systems **1-N3O2** and **1-O5** we have maintained the same coordination environment at the axial positions as in **1** but the equatorial ligand $\mathbf{L^{N5}}$ has been modified *in silico* to L^{N3O2} and the 16-crown-5 ligand (*i.e.*, the closest candidate of the crown ether family to the $\mathbf{L^{N5}}$) (Fig. S16 and S17, ESI†). Firstly, we modified *in silico* $\mathbf{L^{N5}}$ (Schiff base ligand formed from 2,6-diacetylpyridine and *N*,*N*′-bis-(3-aminopropyl)-ethylendiamine, see Scheme 1) to L^{N3O2} (Schiff base ligand formed from 2,6-diacetylpyridine and 3,3′-(ethane-1,2-diylbis(oxy))bis(propan-1-amine)). This is an alternative strategy to replace the two –NH– groups that have the larger LoProp charges, with two oxygen groups (Fig. S16, ESI†). In the model system **1-N3O2** (Fig. S16, ESI†) the first excited state is calculated at 658 K (m_J = ±13/2, g_{zz} = 17.046, g_{xx} = 0.028, g_{yy} = 0.032) with the second (m_J = ±11/2) located at 1190 K and the third ($0.62|\pm1/2> + 0.22|\pm3/2>$) excited state at 1438 K (Table S6, ESI†). The maximum calculated relaxation barrier, U_{cal}, for model system **1-N3O2** is estimated at ~1400 K (Fig. 4, upper). In addition, the computed LoProp charges on the oxygen atoms are found to be 50% smaller than those on the –NH– groups in **1** (Fig. S18, ESI†). Next we employed a crown ether ligand in the equatorial plane of our model system because of its neutral nature, long metal–ligand distances, the popularity of crown ether ligands in 4f chemistry[24] and to compare it with $\mathbf{L^{N5}}$ and L^{N3O2}. In the model system **1-O5** the strongly axial excited states are higher in energy than that of **1** (Table S7, ESI†). In addition, the transverse components for model system **1-O5** are weaker giving lower g_{xx}/g_{yy} values (Table S7, ESI†). The QTM probabilities calculated for the first three KDs (0.45×10^{-4}, 0.49×10^{-2}, $0.68 \times 10^{-1}\mu_B$, respectively) are lower compared to **1** with the magnetization relaxing *via* the fourth KD giving a calculated magnetization reversal barrier of 1788 K (Fig. 4, lower). The ratio between the axial B_2^0 parameter and the corresponding non-axial crystal field parameters also increases **1** < **1-N3O2** < **1-O5** (Table S8, ESI†) supporting the increase of U_{cal} from **1** (~1040 K) to **1-N3O2** (~1400 K) and **1-O5** (~1800 K) (Fig. S20, ESI†).

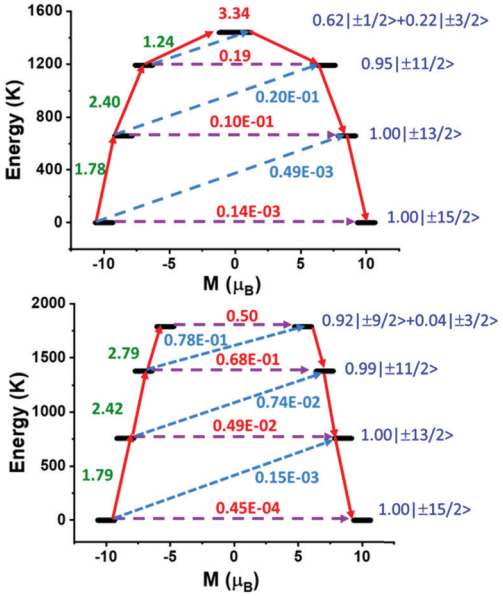

Fig. 4 *Ab initio* calculated relaxation dynamics for **1-N3O2** (Upper) and **1-O5** (Lower). The black line indicates the KDs as a function of magnetic moments. The violet dashed arrow represents QTM (QTM = quantum tunnelling of the magnetisation) *via* the ground state and TA-QTM (TA-QTM = thermally assisted QTM) *via* excited states. The blue dashed arrow indicates possible Orbach processes. The red arrows indicate the mechanism of magnetic relaxation (Orbach/Raman). The numbers above each arrow represent corresponding transverse matrix elements for the transition magnetic moments.[25]

In conclusion, we report $[Dy^{III}(\mathbf{L^{N5}})(Ph_3SiO)_2](BPh_4)\cdot CH_2Cl_2$ (**1**) using the macrocyclic ligand $\mathbf{L^{N5}}$, which is a strongly axial Dy(III) single-ion magnet in a pentagonal bipyramidal geometry showing out-of-phase peaks up to 80 K under zero field, a high anisotropy barrier of 1108 K, and hysteresis loops open up to 14 K (@ 0.01 T s^{-1}). This novel compound was engineered following our flexible synthetic approach where five long Dy–N bonds are formed by the macrocyclic ligand $\mathbf{L^{N5}}$, while two strong donor Ph_3SiO^- ligands are used for the axial positions, creating the short O–Dy–O bonds. Future work will involve modifying the planarity and rigidity of the $\mathbf{L^{N5}}$ macrocycle and investigating the new pentagonal bipyramidal families

identified through our computational studies, showing the vast scope for macrocyclic engineering of magnetic anisotropy.

We thank EPSRC UK (EP/N01331X/1, EP/M000923/1) for funding. S. D. thanks UGC for an SRF fellowship. G. R. thanks DST/SERB for funding (CRG/2018/000430; DST/SJF/CSA03/2018-10; SB/SJF/2019-20/12).

Conflicts of interest

There are no conflicts to declare.

Notes and references

1 S. M. J. Aubin, M. W. Wemple, D. M. Adams, H.-L. Tsai, G. Christou and D. N. Hendrickson, *J. Am. Chem. Soc.*, 1996, **118**, 7746; R. Sessoli, H. L. Tsai, A. R. Schake, S. Wang, J. B. Vincent, K. Folting, D. Gatteschi, G. Christou and D. N. Hendrickson, *J. Am. Chem. Soc.*, 1993, **115**, 1804; C. J. Milios, A. Vinslava, W. Wernsdorfer, S. Moggach, S. Parsons, S. P. Perlepes, G. Christou and E. K. Brechin, *J. Am. Chem. Soc.*, 2007, **129**, 2754.

2 A. Castro-Alvarez, Y. Gil, L. Llanos and D. Aravena, *Inorg. Chem. Front.*, 2020, **7**, 2486; M. J. Heras Ojea, L. H. C. Maddock and R. A. Layfield, *Lanthanide Organometallics as Single-Molecule Magnets*, Springer, New York, NY, 2019, vol. 64; F.-S. Guo and R. A. Layfield, *Acc. Chem. Res.*, 2018, **51**, 1880; M. Feng and M.-L. Tong, *Chem. – Eur. J.*, 2018, **24**, 7574; A. K. Bar, P. Kalita, M. K. Singh, G. Rajaraman and V. Chandrasekhar, *Coord. Chem. Rev.*, 2018, **367**, 163.

3 S. Bala, G.-Z. Huang, Z.-Y. Ruan, S.-G. Wu, Y. Liu, L.-F. Wang, J.-L. Liu and M.-L. Tong, *Chem. Commun.*, 2019, **55**, 9939; J. Wu, J. Jung, P. Zhang, H. Zhang, J. Tang and B. Le Guennic, *Chem. Sci.*, 2016, **7**, 3632; K. Katoh, S. Yamashita, N. Yasuda, Y. Kitagawa, B. K. Breedlove, Y. Nakazawa and M. Yamashita, *Angew. Chem., Int. Ed.*, 2018, **57**, 9262.

4 P. Zhang, L. Zhang, C. Wang, S. Xue, S.-Y. Lin and J. Tang, *J. Am. Chem. Soc.*, 2014, **136**, 4484; K. L. M. Harriman, J. L. Brosmer, L. Ungur, P. L. Diaconescu and M. Murugesu, *J. Am. Chem. Soc.*, 2017, **139**, 1420; S.-M. Chen, Y.-Q. Zhang, J. Xiong, B.-W. Wang and S. Gao, *Inorg. Chem.*, 2020, **59**, 5835.

5 A. B. Canaj, M. K. Singh, C. Wilson, G. Rajaraman and M. Murrie, *Chem. Commun.*, 2018, **54**, 8273.

6 Y.-C. Chen, J.-L. Liu, L. Ungur, J. Liu, Q.-W. Li, L.-F. Wang, Z.-P. Ni, L. F. Chibotaru, X.-M. Chen and M.-L. Tong, *J. Am. Chem. Soc.*, 2016, **138**, 2829; Y.-S. Ding, N. F. Chilton, R. E. P. Winpenny and Y.-Z. Zheng, *Angew. Chem., Int. Ed.*, 2016, **55**, 16071; J. Liu, Y.-C. Chen, J.-L. Liu, V. Vieru, L. Ungur, J.-H. Jia, L. F. Chibotaru, Y. Lan, W. Wernsdorfer, S. Gao, X.-M. Chen and M.-L. Tong, *J. Am. Chem. Soc.*, 2016, **138**, 5441; Y. Ma, Y.-Q. Zhai, Y.-S. Ding, T. Han and Y. Z. Zheng, *Chem. Commun.*, 2020, **56**, 3979; J. L. Liu, Y. C. Chen, Y. Z. Zheng, W. Q. Lin, L. Ungur, W. Wernsdorfer, L. F. Chibotaru and M. L. Tong, *Chem. Sci.*, 2013, **4**, 3310; Y.-S. Ding, T. Han, Y.-Q. Zhai, D. Reta, N. F. Chilton, R. E. P. Winpenny and Y.-Z. Zheng, *Chem. – Eur. J.*, 2020, **26**, 5893; S. K. Gupta, T. Rajeshkumar, G. Rajaraman and R. Murugavel, *Chem. Sci.*, 2016, **7**, 5181.

7 A. B. Canaj, S. Dey, E. Regincós Martí, C. Wilson, G. Rajaraman and M. Murrie, *Angew. Chem., Int. Ed.*, 2019, **58**, 14146; A. B. Canaj, S. Dey, E. Regincós Martí, C. Wilson, G. Rajaraman and M. Murrie, *Angew. Chem.*, 2019, **131**, 14284.

8 Z.-H. Li, Y.-Q. Zhai, W.-P. Chen, Y.-S. Ding and Y.-Z. Zheng, *Chem. – Eur. J.*, 2019, **25**, 16219.

9 S. Demir, M. I. Gonzalez, L. E. Darago, W. J. Evans and J. R. Long, *Nat. Commun.*, 2017, **8**, 2144.

10 P. Evans, D. Reta, G. F. Whitehead, N. F. Chilton and D. P. Mills, *J. Am. Chem. Soc.*, 2019, **141**, 19935.

11 C. Gould, K. R. McClain, J. Yu, T. J. Groshens, F. Furche, B. G. Harvey and J. R. Long, *J. Am. Chem. Soc.*, 2019, **141**, 12967.

12 A. P. Goodwin, F. Ortu, D. Reta, N. F. Chilton and D. P. Mills, *Nature*, 2017, **548**, 439; F.-S. Guo, B. M. Day, Y.-C. Chen, M.-L. Tong, A. Mansikkamaki and R. A. Layfield, *Angew. Chem., Int. Ed.*, 2017, **56**, 11445.

13 K. R. McClain, C. A. Gould, K. Chakarawet, S. J. Teat, T. J. Groshens, J. R. Long and B. G. Harvey, *Chem. Sci.*, 2018, **9**, 8492.

14 F.-S. Guo, B. M. Day, Y.-C. Chen, M.-L. Tong, A. Mansikkamäki and R. A. Layfield, *Science*, 2018, **362**, 1400.

15 L. Spree and A. A. Popov, *Dalton Trans.*, 2019, **48**, 2861; W. Yang, G. Velkos, F. Liu, S. M. Sudarkova, Y. Wang, J. Zhuang, H. Zhang, X. Li, X. Zhang, B. Büchner, S. M. Avdoshenko, A. A. Popov and N. Chen, *Adv. Sci.*, 2019, 1901352; G. Velkos, W. Yang, Y.-R. Yao, S. M. Sudarkova, X. Liu, B. Büchner, S. M. Avdoshenko, N. Chen and A. A. Popov, *Chem. Sci.*, 2020, **11**, 4766; Y. Wang, J. Xiong, J. Su, Z. Hu, F. Ma, R. Sun, X. Tan, H.-L. Sun, B.-W. Wang, Z. Shi and S. Gao, *Nanoscale*, 2020, **12**, 11130.

16 A. B. Canaj, M. K. Singh, E. Regincós Martí, M. Damjanović, C. Wilson, O. Céspedes, W. Wernsdorfer, G. Rajaraman and M. Murrie, *Chem. Commun.*, 2019, **55**, 5950.

17 A. B. Canaj, S. Dey, C. Wilson, O. Céspedes, G. Rajaraman and M. Murrie, *Chem. Commun.*, 2020, **56**, 1533.

18 J. Li, S. Gómez-Coca, B. S. Dolinar, L. Yang, F. Yu, M. Kong, Y.-Q. Zhang, Y. Song and K. R. Dunbar, *Inorg. Chem.*, 2019, **58**, 2610; Q.-W. Li, R.-C. Wan, Y.-C. Chen, J.-L. Liu, L.-F. Wang, J.-H. Jia, N. F. Chilton and M.-L. Tong, *Chem. Commun.*, 2016, **52**, 13365; W. Zhao, H. Cui, X.-Y. Chen, G. Yi, L. Chen, A. Yuan and C.-L. Luo, *Dalton Trans.*, 2019, **48**, 5621.

19 S. M. Nelson, S. G. McFall, M. G. B. Drew, A. H. Bin Othman and N. B. Mason, *J. Chem. Soc., Chem. Commun.*, 1977, 167.

20 M. Pinsky and D. Avnir, *Inorg. Chem.*, 1998, **37**, 5575; D. Casanova, P. Alemany, J. M. Bofill and S. Alvarez, *Chem. – Eur. J.*, 2003, **9**, 1281.

21 D. Gatteschi, R. Sessoli and J. Villain, *Molecular Nanomagnets*, Oxford University Press, Oxford, 2006.

22 K. N. Shrivastava, *Phys. Status Solidi B*, 1983, **117**, 437; S. Q. Wu, Y. Miyazaki, M. Nakano, S. Q. Su, Z. S. Yao, H. Z. Kou and O. Sato, *Chem. – Eur. J.*, 2017, **23**, 10028; A. Singh and K. N. Shrivastava, *Phys. Status Solidi B*, 1979, **95**, 273; A. Chiesa, F. Cugini, R. Hussain, E. Macaluso, G. Allodi, E. Garlatti, M. Giansiracusa, C. A. P. Goodwin, F. Ortu, D. Reta, J. M. Skelton, T. Guidi, P. Santini, M. Solzi, R. De Renzi, D. P. Mills, N. F. Chilton and S. Carretta, *Phys. Rev. B*, 2020, **101**, 174402.

23 A. A. Granovsky, *J. Chem. Phys.*, 2011, **134**, 214113; F. Aquilante, J. Autschbach, R. K. Carlson, L. F. Chibotaru, M. G. Delcey, L. De Vico, I. Fdez Galvan, N. Ferre, L. M. Frutos and L. Gagliardi, *et al.*, *J. Comput. Chem.*, 2016, **37**, 506; L. F. Chibotaru and L. Ungur, *J. Chem. Phys.*, 2012, **137**, 064112.

24 Y. Gil, L. Llanos, P. Cancino, P. Fuentealba, A. Vega, E. Spodine and D. Aravena, *J. Phys. Chem. C*, 2020, **124**, 5308; Y.-S. Ding, T. Han, H. Yue-Qiao, X. Minwei, Y. Sen and Z. Yan-Zheng, *Inorg. Chem. Front.*, 2016, **3**, 798; M. Xemard, M. Cordier, F. Molton, C. Duboc, B. Le Guennic, O. Maury, O. Cador and G. Nocton, *Inorg. Chem.*, 2019, **58**, 2872.

25 L. Ungur, M. Thewissen, J. P. Costes, W. Wernsdorfer and L. F. Chibotaru, *Inorg. Chem.*, 2013, **52**, 6328.

26 L. Gagliardi, R. Lindh and G. Karlstrom, *J. Chem. Phys.*, 2004, **121**, 4494.

